

Molecular cloning, expression and catalytic activity of a human AKR7 member of the aldo–keto reductase superfamily: evidence that the major 2-carboxybenzaldehyde reductase from human liver is a homologue of rat aflatoxin B₁-aldehyde reductase

Linda S. IRELAND*, David J. HARRISON†, Gordon E. NEAL‡ and John D. HAYES*¹

*Biomedical Research Centre, Ninewells Hospital and Medical School, University of Dundee, Dundee DD1 9SY, Scotland, U.K., †Sir Alastair Currie Cancer Research Campaign Laboratories, Department of Pathology, University of Edinburgh, Edinburgh EH8 9AG, Scotland, U.K., and ‡Medical Research Council Toxicology Unit, Hodgkin Building, University of Leicester, P.O. Box 138, Leicester LE1 9HN, U.K.

The masking of charged amino or carboxy groups by N-phthalidyl and O-phthalidyl groups has been used to improve the absorption of many drugs, including ampicillin and 5-fluorouracil. Following absorption of such prodrugs, the phthalidyl group is hydrolysed to release 2-carboxybenzaldehyde (2-CBA) and the pharmaceutically active compound; in humans, 2-CBA is further metabolized to 2-hydroxymethylbenzoic acid by reduction of the aldehyde group. In the present work, the enzyme responsible for the reduction of 2-CBA in humans is identified as a homologue of rat aflatoxin B₁-aldehyde reductase (rAFAR). This novel human aldo–keto reductase (AKR) has been cloned from a liver cDNA library, and together with the rat protein, establishes the AKR7 family of the AKR superfamily. Unlike its rat homologue, human AFAR (hAFAR) appears to be constitutively expressed in human liver, and is widely expressed

in extrahepatic tissues. The deduced human and rat protein sequences share 78 % identity and 87 % similarity. Although the two AKR7 proteins are predicted to possess distinct secondary structural features which distinguish them from the prototypic AKR1 family of AKRs, the catalytic- and NADPH-binding residues appear to be conserved in both families. Certain of the predicted structural features of the AKR7 family members are shared with the AKR6 β -subunits of voltage-gated K⁺-channels. In addition to reducing the dialdehydic form of aflatoxin B₁-8,9-dihydrodiol, hAFAR shows high affinity for the γ -aminobutyric acid metabolite succinic semialdehyde (SSA) which is structurally related to 2-CBA, suggesting that hAFAR could function as both a SSA reductase and a 2-CBA reductase *in vivo*. This hypothesis is supported in part by the finding that the major peak of 2-CBA reductase activity in human liver co-purifies with hAFAR protein.

INTRODUCTION

The importance of the threat posed by aldehydes and ketones to cellular function is emphasized by the fact that a number of separate enzyme systems have evolved that can detoxify these compounds, including aldo–keto reductase (AKR) [1], aldehyde dehydrogenase [2], aldehyde oxidase [3], alcohol dehydrogenase [4], carbonyl reductase [5], quinone reductase [6] and glutathione S-transferase [7]. AKRs are an expanding superfamily of enzymes which currently comprises seven families (AKR1–AKR7) [8]. Mammalian AKRs are found predominantly in the AKR1 family, which includes aldose reductase (ALDR), aldehyde reductase, chlordecone reductase, 3 α -hydroxysteroid dehydrogenase [3 α -HSD; also sometimes referred to as dihydrodiol dehydrogenase (DD)], and Δ^4 -3 oxosteroid 5 β -reductase [9–17]. In addition to these enzymes, a separate distantly related protein has been described in rat liver that catalyses the NADPH-dependent reduction of a dialdehydic metabolite of the hepatocarcinogen aflatoxin B₁ (AFB₁) [18,19]. This aflatoxin-metabolizing aldehyde reductase from rat liver has been designated aflatoxin B₁-aldehyde reductase (AFAR), and because it shares less than 25 % identity with the AKR1 family, it has been

recently designated as the founding member of the AKR7 family [8]. The remaining mammalian AKR superfamily members are all β -subunits of the *Shaker*-related voltage-gated K⁺-channels [20–23], and collectively form the AKR6 family [8] (at present, all the AKR2–AKR5 members that have been identified are from plants, yeast and bacteria [8]). These AKR6 proteins show more similarity to AFAR than to the AKR1 family reductases [24]. The significance of the structural similarity between AFAR and the K⁺-channel β -subunits is not known and, to date, the ability of AKR6 proteins to catalyse oxidoreductase reactions has not been demonstrated.

The biotransformation of aldehydes and ketones depends both on the structure of the chemical in question, and on the level of expression of the various carbonyl-metabolizing enzymes. In mammalian species, aldehydes are primarily oxidized to carboxy derivatives, whereas ketones are reduced to secondary alcohols [25]. An exception to this generalization is provided by 2-carboxybenzaldehyde (2-CBA), or *O*-phthalaldehydic acid, which is extensively reduced to the corresponding alcohol in many species, including rat, mouse, rabbit, dog and monkey [26]; this carbonyl-containing compound is of interest to the pharmaceutical industry because it is used to mask drugs and enhance

Abbreviations used: ALDR, aldose reductase; AFAR, aflatoxin B₁-aldehyde reductase; AFB₁, aflatoxin B₁; 2-CBA, 2-carboxybenzaldehyde; AKR, aldo–keto reductase; DD, dihydrodiol dehydrogenase; DTT, dithiothreitol; GABA, γ -aminobutyric acid; 3 α -HSD, 3 α -hydroxysteroid dehydrogenase; ORF, open reading frame; Pefabloc, 4-(2-aminoethyl)-benzenesulphonyl fluoride hydrochloride; 9,10-PQ, 9,10-phenanthrenequinone; SSA, succinic semialdehyde; 4-NBA, 4-nitrobenzaldehyde; UTR, untranslated region.

The cDNA sequence for human AFAR has been assigned by GenBank the accession number AF026947.

¹ To whom correspondence should be addressed.

their delivery to target sites [27,28]. Most significantly, 2-CBA has been administered to a human volunteer, and 76% of the 50 mg oral dose was recovered within 24 h in the urine as the alcohol derivative [29]. The enzyme responsible for the reduction of 2-CBA in human liver has not been identified, although the 2-CBA reductase in rat liver has been partially characterized, and is thought to be an AKR [30,31].

In the present paper, we describe the molecular cloning of a human AKR that shares 78% identity with rat AFAR (rAFAR), but less than 25% identity with human AKR1 family members. The human AKR with homology to rat AFAR has been designated hAFAR, because it is not only structurally related to rAFAR, but can also catalyse conversion of the dialdehydic form of AFB₁ into the dialcoholic form. From an initial screen of AKR substrates, it has been found that hAFAR has high affinity for the γ -aminobutyric acid (GABA) metabolite succinic semi-aldehyde (SSA), and further investigation of carbonyl-containing compounds similar to SSA and AFB₁ dialdehyde has shown that 2-CBA is an excellent substrate for both human and rat recombinant AFAR enzymes. Resolution of the various AKR iso-enzymes from human liver by anion-exchange chromatography has demonstrated that the major peak of 2-CBA reductase activity co-purifies with AFAR protein, strongly suggesting that this enzyme is primarily responsible for the metabolism *in vivo* of 2-CBA.

MATERIALS AND METHODS

Reagents

Chemicals and enzymes were of the highest grade and were readily available commercially. A human liver cDNA library, in the Unizap XR vector, was from Stratagene (La Jolla, CA, U.S.A.), and the multiple-tissue Northern blots were from Clontech (Palo Alto, CA, U.S.A.). The Sequenase Version 2.0 kit for DNA sequencing was supplied by Amersham International (Slough, Berks., U.K.). The Novagen pET15b expression vector and thrombin were purchased from AMS Biotechnology U.K. (Oxon, U.K.). Pefabloc [4-(2-aminoethyl)-benzenesulphonyl fluoride hydrochloride], a serine protease inhibitor, was purchased from Boehringer Mannheim (Lewes, East Sussex, U.K.). The Matrex gel Orange A was from Amicon (Stonehouse, Glos., U.K.), and the HiTrap Blue, HiTrap Chelating and Q-Sepharose columns were from Pharmacia Biosystems Ltd (Milton Keynes, Herts., U.K.).

Human tissue

Specimens of human liver were obtained with formal consent (for full autopsy and the removal of tissues for teaching and research). They were collected less than 15 h after death, and frozen at -70°C immediately following removal from cadavers. Column chromatography was performed on liver 666 from an 82-year-old Caucasian male who died from an aortic aneurysm; this specimen appeared normal on histological examination.

Molecular cloning and Northern blotting

The human cerebellum and liver cDNA libraries were screened with 50-mer oligonucleotides complementary to either EST00883 [32] or the mid-coding region of hAFAR. The libraries were plated out on *Escherichia coli* XL-1 Blue MRF' cells and positive plaques identified, using standard techniques [33], by hybridization with [γ -³²P]ATP-labelled oligonucleotide at 49°C in 20 mM sodium phosphate buffer, pH 7.0, which contained $3 \times \text{SSC}$ (where $1 \times \text{SSC}$ is 0.15 M NaCl/0.015 M sodium citrate),

$10 \times \text{Denhardt's}$ (0.02% Ficoll 400/0.02% polyvinylpyrrolidone/0.002% BSA), 100 mg/ml salmon sperm DNA and 7% (w/v) SDS; membranes were washed at 65°C in a solution containing $6 \times \text{SSC}$, 0.05% (w/v) pyrophosphate and 1% (w/v) SDS to remove non-specifically bound probe. Once plaque-pure, phagemid excision and isolation of single-stranded DNA was performed according to the protocol accompanying the libraries. Sequence analysis of the clones isolated from the human brain and liver cDNA libraries was achieved by dideoxy chain-termination reactions [34].

The human AFAR coding sequence (in pLI16) was amplified by PCR using the two oligonucleotides 5'-GGGAATTCCAT-ATGTCCCGGCCACCGCCACCGC-3' (sense) and 5'-CCCT-TCTAAGTCAGCTCGAGGCCAAGACTGGTTCAGTGTG-3' (antisense) to introduce 5' *EcoRI* and *NdeI* sites and a 3' *XhoI* site. The amplified DNA was digested with *EcoRI* and *XhoI* before ligation with similarly treated pBluescript SK+. The ligated PCR product (pLI18) was used to transform *E. coli* NM522 cells, and the DNA insert sequenced to verify the fidelity of amplification.

Northern blots of mRNA, using the pre-size-fractionated human tissue blots supplied by Clontech, were probed with the *EcoRI/BglII* fragment of pLI18, according to the instructions of the supplier. To check for integrity of the RNA, as well as amounts loaded, the blots were probed with a 2.0 kb human β -actin cDNA that was also supplied by Clontech.

Computer-aided sequence and structural analyses of AFAR

Comparison between the nucleotide sequence of pLI16 and other cDNAs was carried out by Blast search of Genbank database [35]. From the deduced primary structure of the human AFAR protein, predictions of its secondary structure were made using the PHD profile-network method [36,37]. This information was compared with the known secondary structures of ALDR [38,39] entered in the Brookhaven database.

Bacterial expression and isolation of recombinant AFAR

The coding region for hAFAR was excised from pLI18 by digestion with *NdeI* and *XhoI*, and ligated into the pET15b expression vector, which had been treated with the same restriction enzymes. Ligated DNA was used to transform *E. coli* BL21 pLysS, and the hAFAR expression construct (pLI19) was selected for on Luria broth agar plates containing ampicillin (0.1 mg/ml) and chloramphenicol (0.034 mg/ml). Expression of recombinant His-tagged hAFAR protein was induced for 2.5 h at 37°C by addition of 1 mM isopropyl β -D-thiogalactoside to mid-exponential-phase pLI19-transformed BL21pLysS cells. These cells were harvested by centrifugation, frozen at -70°C , and lysed in 20 mM Tris/HCl buffer, pH 7.9, containing 5 mM imidazole and 500 mM NaCl (buffer A). Lysates were filtered through a 0.45 μm Whatman polysulphone disc, and recombinant hAFAR was isolated by charging the filtered material on to a 5 ml HiTrap Chelating column pre-equilibrated with buffer A. After washing, recombinant polyhistidine-tagged protein was recovered by elution of the HiTrap Chelating column with 200 mM imidazole in buffer A. The polyhistidine tag was removed from the recombinant protein by cleavage (2 h, 25°C) with thrombin (1 unit per mg of hAFAR) in 20 mM Tris/HCl, pH 8.3/2.5 mM CaCl₂. Thrombin-cleaved protein was diluted by addition of 3 vol. of 50 mM Tris/HCl, pH 6.8/0.1% (v/v) NP40 and loaded on to a 1 ml HiTrap Blue column equilibrated with 20 mM Tris/HCl, pH 7.0, containing 50 mM NaCl and 0.1% (v/v) NP40. Recombinant hAFAR was eluted from the

HiTrap Blue column with 4 mM NADPH in 100 mM Tris/HCl, pH 8.3, containing 1.5 M NaCl and 0.1% (v/v) NP40, and dialysed against 100 mM sodium phosphate, pH 6.8. Finally, hAFAR was diluted with an equal vol. of dialysis buffer containing 10% (v/v) glycerol and frozen at -70°C until required.

Recombinant rAFAR, expressed in *E. coli* BL21pLysS from pEE65, was isolated from bacterial cultures as described previously [40].

Protein determination

This was carried out by the method of Bradford [41].

SDS/PAGE

SDS/PAGE was performed in 12% polyacrylamide resolving gels with the buffer system described by Laemmli [42].

Amino-acid sequencing

Peptides from hAFAR were resolved either by reversed-phase HPLC or by SDS/PAGE; in the latter case, the separated peptides were electroblotted on to ProBlott[®] membranes supplied by Applied Biosystems, and were detected by Ponceau S staining. Sequencing of peptides was carried out as previously described [43] using an Applied Biosystems 477A instrument with an on-line phenylthiohydantoin analyser.

Electrospray MS of cleaved human AFAR

This was carried out with a Finnigan Mat Lasermat instrument as described previously [18].

Reductase activity towards AFB₁-dialdehyde

The substrate for AFAR, the dialdehydic form of AFB₁-8,9-dihydrodiol, is the hydrolysis product of the unstable 8,9-epoxide. In this study, we added pre-prepared AFB₁-8,9-dihydrodiol directly to incubations with recombinant hAFAR and rAFAR, rather than generating the dihydrodiol by microsomal metabolism of AFB₁ in the presence of AFAR. By this means, we ensured that throughout the incubations with AFAR there was an excess of AFB₁-dihydrodiol present.

The first stage in the assay involved the catalytic NADPH-dependent formation of AFB₁-8,9-epoxide, which rapidly undergoes hydrolysis to produce AFB₁-8,9-dihydrodiol. NADPH was generated in a preincubation of NADP⁺ (1.65 μmol), glucose 6-phosphate (23.6 μmol), potassium phosphate buffer, pH 7.4, (305 μmol) MgCl₂, (19.1 μmol) and glucose-6-phosphate dehydrogenase (1.2 units) in a total vol. of 2.14 ml. Incubations were carried out at 37°C for 5 min to generate NADPH, followed by addition of AFB₁ (154 nmol in 24 μl of DMSO) and washed quail-liver microsomes (600 μl of a suspension in 150 mM KCl, containing microsomes equivalent to 375 mg of liver). The AFB₁-dihydrodiol was then generated by incubation at 37°C for 30 min with continuous gentle shaking, followed by centrifugation (100000 g for 30 min) to remove microsomes. The resulting supernatant (approx. 2.6 ml) containing AFB₁-dihydrodiol was shown to contain no residual AFB₁. The NADPH-generating system was replenished by the further addition of glucose 6-phosphate (23.6 μmol), NADP⁺ (1.65 μmol) and glucose-6-phosphate dehydrogenase (1.2 units). Aliquots (170 μl) of the AFB₁-dihydrodiol-containing solution were added to samples of hAFAR (75 μg of protein in 50 μl of 20 mM

sodium phosphate buffer, pH 7.0) and rAFAR (16.5 μg of protein in 33 μl of 20 mM sodium phosphate buffer, pH 7.0) and the total vol. of the incubations brought to 250 μl by the addition of distilled water. Catalytic reduction of AFB₁-dialdehyde was carried out for 10 min at 37°C . The reactions were carried out in triplicate, with gentle shaking, and terminated by the transfer of the tubes to ice, followed by the addition of ice-cold methanol (1 ml). Further sample processing was performed as described previously [44]. The AFB₁ metabolites were separated by HPLC on a 3 mm \times 100 mm cartridge Chromspher 5 C₁₈ column (Chrompack, The Netherlands) using a linear 15%–40% methanol gradient containing aq. 8% (v/v) acetonitrile and 0.02% (w/v) phosphoric acid throughout. The column was developed over 7 min at a flow rate of 1 ml/min. AFB₁ metabolites were detected by monitoring absorbance at 365 nm, and the fluorescence at 405 nm.

AKR activity towards model substrates

The screening of carbonyl-containing compounds as possible substrates for hAFAR was performed with 1 mM test compound, 0.2 mM NADPH and approximately 15 μg of enzyme, using a Cobas Fara centrifugal analyser (Hoffmann-La Roche Ltd, Basel, Switzerland) to monitor the decrease in absorbance at 340 nm caused by the oxidation of the cofactors NADPH or NADH. Initial velocities (corrected for non-enzymic rates) were determined at 25°C in 100 mM sodium phosphate buffer, pH 6.7 in 250 μl reaction mixtures containing a maximum of either 4% (v/v) acetonitrile, DMSO or methanol. Compounds for which AFAR possessed a specific activity of greater than 0.1 $\mu\text{mol}/\text{min}$ per mg under these standard assay conditions were studied further by determination of K_m and V_{max} values. This was carried out by measuring initial reaction velocities with concentrations of substrate between $0.1 \times K_m$ and $10 \times K_m$, whilst the concentration of cofactor was held at 0.2 mmol/l for either NADPH or NADH. Kinetic parameters were determined by employing the Ultrafit curve-fitting software (Biosoft, Cambridge, U.K.) to fit the Michaelis–Menten equation using the Marquardt algorithm.

Analysis of column eluate was carried out with SSA and 4-nitrobenzaldehyde (4-NBA) under standard assay conditions (i.e. 1 mM substrate and 0.2 mM NADPH, pH 6.7) [45,46]. However, because of its limited solubility, reductase activity towards 9,10-phenanthrenequinone (9,10-PQ) was determined using 0.05 mM substrate in buffer containing 4% (v/v) acetonitrile [47]. Reductase activity towards 2-CBA was initially determined using 1.0 mM substrate [31], but this was reduced to 0.5 mM substrate as higher concentrations were found to be inhibitory.

Purification of AFAR from human liver

Portions (30 g) of human liver were diced and allowed to thaw at 4°C before being homogenized in 150 ml of ice-cold 10 mM Tris/HCl, pH 8.2/0.5 mM dithiothreitol (DTT) (buffer B), containing 0.5 mg/ml Pefabloc. The 100000 g supernatant (cytosol) was prepared at 4°C , and dialysed for 18 h against 3 changes, each of 2 l, of buffer B. The soluble material was applied at 30 ml/h to a 2.5 cm \times 45.0 cm column of Q-Sepharose that was equilibrated and eluted with buffer B. After 250 ml was collected, the anion exchanger was developed with a linear 0–250 mM NaCl gradient formed in 1200 ml of buffer B, that was followed immediately by stepped elution with 1 M NaCl in the same buffer to allow recovery of strongly anionic material. Fractions from Q-Sepharose with AKR activity and cross-

hAFAR	-77	ccgcgtctcgcgtagctctccgcgcgcgcgcgctccactgcgcgcttgcgctctccgcgcgcgcgagccgcgcgctgcgc	-1
rAFAR	-67	gaattc-g-ggc-----aa-----t--cttac-cg-cac--t--tt-tg--acct-tac-a--g--a--	-1
hAFAR	ATG TOC CGG CCA CCG CCA CCG CGG GTC GCC TCG GTG CTG GGC ACC ATG GAG ATG GGG CGC CGC ATG GAC		69
rAFAR	--- --G -AA G-C --- CCT --- A-T --- --- --T G-- --- --- --- --T --- --- --- --T		60
hAFAR	GCG CCC GCC AGC GCC GCG GGC GTG CGC GCC TTT CTG GAG CGC GGC CAC ACC GAA CTG GAC ACG GCC TTC		138
rAFAR	-T- A-- T-- --- T-- --- T-G --- --- --- --C --- C-- --- --- --- --G --G A-A --- --C --- ---		129
hAFAR	ATG TAC AGC GAC GGC CAG TCC GAG ACC ATC CTG GGC GGC CTG GGG CTC GGG CTG GGC GGT GGC GAC TGC		207
rAFAR	G-- --T GCG A-- --T --- --T --- --- --- --A --A -A- --- --- --- --A --- --- C-C A-- -G- ---		198
hAFAR	AGA GTG AAA ATT GCC ACC AAG GCC AAC CCT TGG GAT GGA AAA TCA CTA AAG CCT GAC AGT GTC CGG TCC		276
rAFAR	-A- --A --- --- --- --- --- --T GC- --A AT- TT- --G --G A-- --G --- --A -C- GA- --T --- -T-		267
hAFAR	CAG CTG GAG ACG TCA TTG AAG AGG CTG CAG TGT CCC CAA GTG GAC CTC TTC TAC CTA CAC ACA CCT GAC		345
rAFAR	--- --- --- --- C-- --- --- --- --- --- --GG --- --- --- --T T-- --- TTT --A ---		336
hAFAR	CAC GGC ACC CCG GTG GAA GAG ACG CTG CAT GCC TGC CAG CGS CTG CAC CAG GAG GGC AAG TTC GTG GAG		414
rAFAR	--- --- --T --T A-A --G --- --C --- --G --- --- --C -AC G-- --T --- --- --- --T --- ---		405
hAFAR	CIT GGC CTC TCC AAC TAT GCT AGC TGG GAA GTG GCC GAG ATC TGT ACC CTC TGC AAG AGC AAT GGC TGG		483
rAFAR	--- --T --G --- --- --TC TC- --- --- --- --T --- --T --- --- --- --- --AA --- --- ---		474
hAFAR	<u>ATC CTG CCC ACT GTG TAC CAG GGC ATG TAC AAC GCC ACC ACC</u> CGG CAG GTG GAA ACG GAG CTC TTC CCC		552
rAFAR	--- A-- --A --- --- --- --- --- --- --- -T- --- A-- --- --- --G --T --- --- --- ---		543
hAFAR	TGC CTC AGG CAC TTT GGA CTG AGG TTC TAT GCC TAC AAC CCT CTG GCT GGG GGC CTG CTG ACT GGC AAG		621
rAFAR	--- --- --A --- --C --- --A --- --- --C --- -T- --- --- T-- --- --- --- --- --- --GA		612
hAFAR	TAC AAG TAT GAG GAC AAG GAC GGG AAA CAG CCT GTG GGC CGC TTC TTT GGG AAT AGC TGG GCT GAG ACC		690
rAFAR	--T --A --C C-- --T --- --T --- --G A-T --- -A- A-- --- --- --- --- --- CCA -TT T-- C-A CTG		681
hAFAR	TAC AGG AAT CGC TTC TGG AAG GAG CAC CAC TTC GAG GCC ATT GCG TTG GTG GAG AAG GCC CTG CAG GCC		759
rAFAR	--- -T- G-C --- -A- --- --- --- G-A --- --- A-T -G- --C --C --- --- --- --T --- A-- A-T		750
hAFAR	GCA TAT GGC GCC AGC GCC CCC AGT GTG ACC TCG GCT GCC CTC CGG TGG ATG TAC CAC CAC TCA CAG CTG		828
rAFAR	A-C --- --- C-- --CT --- --- --- A-- -T- --A --- --- G-A --- --- --- --T --- --- --C		819
hAFAR	CAG GGT GCC CAC GGG GAC GCG GTC ATC CTG GGC ATG TCC AGC CTG GAG CAG CTG GAG CAG AAC TTG GCA		897
rAFAR	A-- --C A-- --A --- --T --A --- --T --- --- --- --- --T --- --A --A --- --- --- --- --C		888
hAFAR	GCA ACA GAG GAA GGG CCC CTG GAG CCG <u>GCT GTC GTG GAT GCC TTT AAT CAA GCC TGG CAT TTG GTT GCT</u>		966
rAFAR	TTG GTC --- --- --- --T --- --- --A --- --T --- --- --- G-C --- --- A-C C-A --- --C		957
hAFAR	<u>CAC GAA TGT</u> CCC AAC TAC TTC CGC tag .gcccatcattggctcaggctgcccaagggtttttctgtoacctotttttctctc		1047
rAFAR	--- --G --- --- --- --T --- --- --a gata----tgccct-gg--a--g-gc--ct-ac-gcc-gc--cgcc----c--...		1036
hAFAR	acaactgaccagtcttgccottaagctgacttagaagggtttttctgaattgtotagatccattatTTTTtagcttctgctgcttctg		1138
rAFAR--g--cg-t----tc-g-ttctt-cc--t-t-gacagg-cac-gtc-ttt-ct-ccc-gotttc-atacagccag-		1112
hAFAR	ccctattoactttacaactgtgaaaggtgggggtgagctcccacttgagcgcttctgttgaataaagcaggcacttgacctgctgtagoc		1229
rAFAR	tg--t-ca-ag-g-g-gctg-ctga-coccaatacctc-tgctgaataaac-gt-ccctgtc-c---ct-gg--ac-a-----g--cc-a		1202
hAFAR	taggtottgagtgaacccccaaaaa		1254

Figure 1 Nucleotide sequence of the cDNA clone for hAFAR

The nucleotide sequence of pL116, encoding hAFAR, was determined by the dideoxynucleotide chain-termination method [34]. Both strands of the cDNA were analysed. The sequence is shown aligned with that of pEE60, which encodes rAFAR [19]; dashed lines in pEE60 represent nucleotides which are shared by the two cDNA clones. A gap has been introduced into pEE60 between nucleotides 10–18 to maximize homology. Capital letters represent those nucleotides encoding protein. Position +1 is the first base in the ATG initiation codon. The two 50-mer oligonucleotides which were used to screen the cerebellum and liver libraries are underlined; oligo-1 is situated closer to the 3'-end of the clone than oligo-2.

reactivity with anti-hAFAR IgG were combined and dialysed against 2 changes, each of 2 l, of 10 mM Tris/HCl, pH 7.6, containing 0.5 mM DTT. The dialysed material was applied to a 1.6 cm × 4.0 cm column of Matrex Orange A, and retained protein was eluted by 20 mM Tris/HCl, 600 mM NaCl buffer, pH 8.3. Finally, the protein-containing fractions eluted from Matrex Orange A that exhibited activity to 2-CBA were combined and applied manually, by syringe, to a 1 ml pre-packed HiTrap Blue dye-affinity gel, and the bound protein was eluted with

10 mM Tris/HCl, pH 8.3, containing 1 mM NADPH and 30% (v/v) acetonitrile.

Immunochemical methods

The AFAR antibodies used in this study were raised in female New Zealand White rabbits against purified heterologously expressed human protein; the immunization schedule employed was that used to raise antibodies against rat AFAR [18].

Antibodies were also raised against heterologously expressed polyhistidine-tagged human 3α -HSD, using the c32 cDNA clone that was isolated from an ethacrynic-acid-resistant HT29 colon-cell line by Ciaccio and Tew [14]. The cDNA encoding 3α -HSD (provided by Dr. Ken D. Tew, Fox Chase Cancer Center, Philadelphia, PA, U.S.A.) was expressed in *E. coli* from the pET15b vector, as described above for AFAR. Western blotting was carried out using a 1:2000 final dilution of either anti-hAFAR IgG or anti-(3α -HSD) IgG. The blots were detected using enhanced chemiluminescence [48].

Immunohistochemistry of AFAR in human liver was carried out on biopsy specimens obtained for diagnostic purposes. A normal liver sample was obtained from a patient about to start methotrexate therapy for psoriasis, and a liver sample with inflammatory disease was from a patient with primary biliary cirrhosis. Immunohistochemistry was performed on formalin-fixed paraffin-embedded 4 μ m sections. Following incubation of de-waxed liver sections with a 1:100 dilution of primary antibody against hAFAR followed by biotinylated goat anti-rabbit second antibody, immunoreactive protein was allowed to react with biotin-streptavidin-horseradish peroxidase, before the complexes were detected using 3,3'-diaminobenzidine as substrate.

RESULTS

Cloning of the human homologue of the rAFAR cDNA

The likely existence of a protein in man that is closely related to

rat AFAR was initially suggested by Ellis et al. [19] who pointed out that a 140 bp region of an expressed sequence tag, EST00883, obtained from human cerebellum by Ventner and his co-workers [32], shares 85% sequence identity with that portion of the rat AFAR cDNA encoding the C-terminal part of the protein. Initial attempts to isolate a full-length version of EST00883 by screening a human cerebellum library using a 50-mer oligonucleotide complementary to the expressed sequence tag (oligo-1; Figure 1) resulted in the isolation of three partial-length cDNAs from the screening of 2×10^5 plaques. The longest of these was approximately 800 bp in length, and appeared to comprise the 3'-half of the cDNA for the putative human AFAR. On the basis of the sequence data obtained from the longest of these clones, a second 50-mer oligonucleotide (oligo-2; Figure 1) was employed which allowed screening for more complete cDNAs. In an attempt to isolate a full-length cDNA, attention was switched from cerebellum to liver; the expression of hAFAR in extrahepatic tissues will be described later. Approximately 4.2×10^5 plaques of a human liver cDNA library were screened using oligo-2. One of four positive clones purified was shown to contain an open reading frame (ORF) homologous to the entire coding region of the rat cDNA. This human cDNA clone, pLI16, comprises 1331 bp and contains a 990 bp ORF which initiates at an ATG triplet located 78 bp from the 5'-end. The rat and human cDNAs were found to share 81% identity over their coding regions (Figure 1). In contrast, the 5'-untranslated regions (UTRs) of these clones share 43% identity,

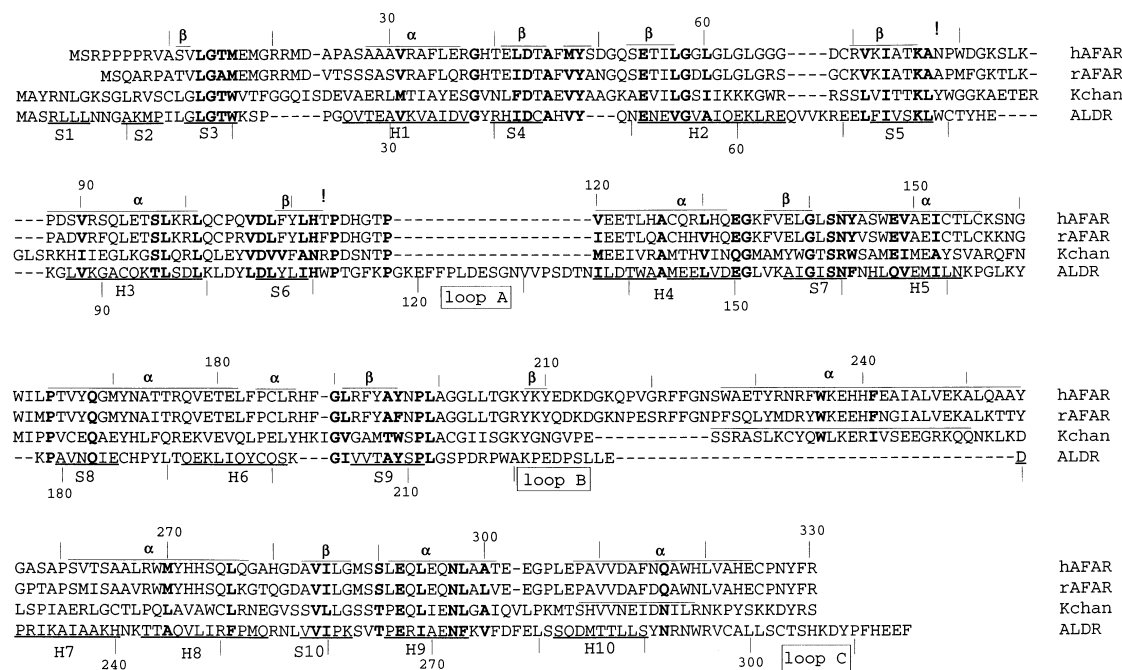


Figure 2 Predicted secondary structural elements of human and rat AFAR proteins

The deduced amino acid sequences of hAFAR (this study) and rAFAR [19] were analysed by the PHD profile network method to allow prediction of regions which adopt α -helix or β -sheet structures; the amino acids comprising these regions are shown by a solid line and an α or β symbol. Such predictions were aligned with those amino acids from ALDR that are known from X-ray crystallography [38,39] to be involved in α -helix (shown as H1–H10) or β -sheet (shown as S1–S10) structures. The numbering of the amino acid residues of hAFAR (shown above sequence) includes the initiator methionine, whereas the numbering of amino acids in ALDR (shown below sequence) excludes the initiator methionine. The *Shaker*-related voltage-gated K^+ -channel β -subunit in human heart (amino acids 78–408) described by England et al. [21] was also included in the line-up because such subunits are thought to be related to the AFAR proteins [24]. Alignment of hAFAR and rAFAR with secondary structural elements of ALDR suggests that many of these elements are conserved. Significantly, these alignments indicate that loop A in ALDR is represented in neither human nor rat AFAR, and that loop B in ALDR is extended in both AFAR proteins. !, residues 78 and 113 in hAFAR, which correspond to critical tryptophans in the substrate-binding site of ALDR (Trp⁷⁹ and Trp¹¹¹).

β subunit K ⁺ channel	22							
Aldehyde Reductase	18	20						
Aldose Reductase	16	19	50					
Delta 4-3 oxosteroid 5- beta reductase	18	17	43	50				
Chlordecone reductase	16	17	40	45	54			
Human aldo-keto reductase B	16	18	38	45	54	84		
c81 dihydrodiol dehydrogenase	18	18	39	46	56	82	87	
c32 dihydrodiol dehydrogenase	18	19	39	45	56	83	88	98
	hAFAR	β subunit K ⁺ channel	Aldehyde Reductase	Aldose Reductase	Delta 4-3 oxosteroid 5-beta reductase	Chlordecone reductase	Human aldo-keto reductase B	c81 dihydrodiol dehydrogenase
	AKR7	AKR6	AKR1A	AKR1B	AKR1D	AKR1C		

Figure 3 Percentage identity between hAFAR and other members of the human AKR superfamily

Sequences were aligned by minimizing disruption to the predicted secondary structure as shown in Figure 2, and % identity determined for each alignment. The protein structure of hAFAR was deduced from pLI16. The amino acid sequences of human AKR were obtained from the Entrez database at NCBI. Genbank accession numbers are as follows: human β -subunit [21], L39833; aldehyde reductase [9], J04794; Δ^4 -3 oxosteroid 5 β -reductase [13], P51857; chlordecone reductase [10], M33375; HAKRb [12], P42330; c32 DD [14], U05684; c81 DD [14], U05598.

whereas their 3'-UTRs share less than 30% identity. The coding region of pLI16 translates to a polypeptide of 330 residues with an estimated molecular mass of 36625 Da (Figure 2). The predicted human protein is three amino acids longer than rat AFAR, the difference in size being due to the insertion of three additional Pro residues (4, 5 and 6) in hAFAR. These additional residues result in an unusual MSRPPPP heptapeptide being produced at the N-terminus of hAFAR. The predicted human and rat protein sequences possess 78% identity and 87% similarity. Among human gene products, the protein encoded by pLI16 shares 22% identity and 35% similarity with the C-terminal 331 amino acids of a β -subunit of voltage-gated K⁺-channel, the most similar member of the AKR superfamily to hAFAR, and 16% identity (22% similarity) with ALDR, the most extensively characterized member of the AKR superfamily (Figure 3).

Demonstration that hAFAR can metabolize aflatoxin

As the ability to reduce the dialdehyde form of AFB₁-8,9-dihydrodiol is a characteristic feature of rAFAR it was considered important to establish whether the human protein encoded by pLI16 shares this activity with its rat homologue. In order to examine this possibility, the cDNA encoding hAFAR was expressed in *E. coli* from pLI19 as a polyhistidine-tagged fusion protein, as described in the Materials and methods section. Recombinant hAFAR protein was purified, and following digestion with thrombin to remove the N-terminal histidine tag, it

was shown to migrate as a single polypeptide during SDS/PAGE with a molecular mass of approx. 38 kDa. Examination of this protein by gel filtration on Superose FPLC indicated it had an apparent native molecular mass of 50 kDa (results not shown).

Using an HPLC assay to measure AFB₁ metabolites (Figure 4), it was found that the heterologously expressed human protein encoded by pLI19 could catalyse the conversion of AFB₁-dialdehyde into the dialcohol form. The human protein exhibited a specific activity towards AFB₁-dialdehyde of 1.24 ± 0.18 nmol/min per mg, whereas rAFAR exhibited a specific activity of 3.55 ± 0.36 nmol/min per mg. Consequently, we have designated the human and rat proteins as hAFAR and rAFAR respectively.

The substrate specificity of rat and human AFAR differs with respect to SSA

The substrate specificity of the rat and human AFAR proteins was initially compared with the prototype AKR substrates SSA, 9,10-PQ and 4-NBA. A comparison of the activity of human and rat AFAR for SSA was particularly interesting, as the human enzyme showed an order of magnitude decrease in K_m for SSA relative to the rat enzyme (15 μ M versus 184 μ M; Table 1). Furthermore, SSA is an endogenous metabolite which shows some structural similarity to the dialdehydic phenolate form of AFB₁-8,9-dihydrodiol; both substrates contain a reactive carbonyl group separated by the same number of carbon atoms from a negatively charged oxygen. The affinity of hAFAR for

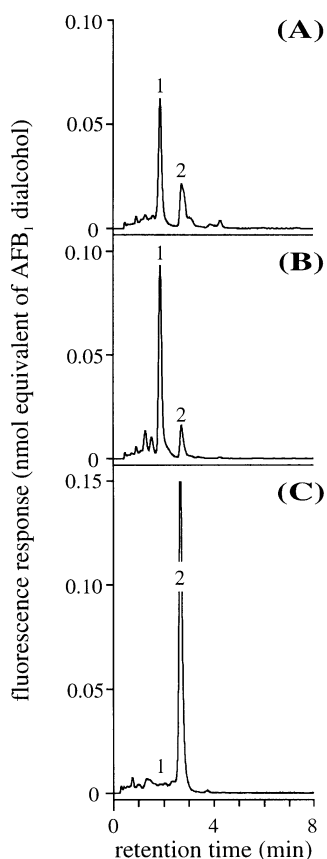


Figure 4 Metabolism of AFB₁-dialdehyde by human and rat AFAR

Purified recombinant human and rat AFAR were incubated in the presence of the dialdehydic form of AFB₁-8,9-dihydrodiol and NADPH at pH 7.4 for 10 min, as described in the Materials and methods section. The reaction was stopped by addition of 1 ml of ice-cold methanol, and the metabolites obtained were resolved on a reversed-phase C₁₈ glass-cartridge system. HPLC eluent was monitored by UV absorption (365 nm) and fluorescence ($\lambda_{\text{excitation}}$ 365 nm, $\lambda_{\text{emission}}$ 405 nm). (A), (B) and (C) show the AFB₁ metabolites produced respectively by hAFAR, rAFAR and a blank control which contained all assay components except AFAR protein. Peak 1 shown is AFB₁-dialcohol, and peak 2 is AFB₁-dialdehyde.

SSA suggested that the structure of SSA might be useful for identifying other potential substrates of hAFAR. A search of the ISIS Database for commercially available compounds [49] that show similarity to SSA led to the identification of 2-CBA as a substrate of hAFAR. The apparent K_m and k_{cat} values of this enzyme for 2-CBA and SSA are similar (Table 1). Under standard assay conditions with NADPH as cofactor, the catalytic efficiency of hAFAR for 2-CBA and SSA is 5×10^6 and $6 \times 10^6 \text{ min}^{-1} \cdot \text{M}^{-1}$ respectively.

Catalytic specificity of hAFAR

A number of commercially available aldehydes that are structurally related to 2-CBA and SSA were examined to characterize further the observed specificity of AFAR for 2-CBA and SSA (Figure 5). Substitution of a keto group by an aldehyde group invariably led to almost complete loss of activity (2-acetylbenzoic acid, 3-benzoylpropionic acid, 9-fluorenone-1-carboxylic acid, 2-benzoylbenzoic acid). The carboxyl group in 2-CBA would appear to be a contributing factor to the metabolism of this compound by hAFAR, as the enzyme had little activity for 2-

methoxybenzaldehyde, and was inactive with 2-hydroxybenzaldehyde. It would be expected that the *o*-hydroxy group should exert a strong electron-withdrawing effect (*o*-effect) resulting in activation of the carbonyl group towards reduction [50], but the fact that hAFAR lacks activity towards 2-hydroxybenzaldehyde suggests that factors other than the reactivity of the carbonyl group determine substrate specificity. It appears to be essential that the carboxyl group of carboxybenzaldehydes is in the *o*-position for reduction by hAFAR because this enzyme is essentially inactive towards both 3-CBA and 4-CBA (Figure 5). This hypothesis is supported by the observation that hAFAR possessed activity towards 2-formylphenoxyacetic acid ($0.9 \mu\text{mol}/\text{min}$ per mg), which like 2-CBA has been reported to be reduced *in vivo* [29].

The initial comparison of human and rat AFAR substrate specificity with the prototype AKR substrates also indicated that both enzymes reduce the bulky hydrophobic α -dicarbonyl compound 9,10-PQ with similar catalytic efficiency (Table 1). The preference of rat AFAR for α -dicarbonyl compounds has been described previously [40], and a search for endogenous dicarbonyl compounds that might be reduced *in vivo* led to the identification of the substrates 16-oxo-oestrone and isatin (Table 1). The oestradiol metabolite, 16-oxo-oestrone, was found to be a good substrate for hAFAR with an apparent K_m of $40 \mu\text{M}$ and k_{cat} of 142 min^{-1} . The endogeneous monoamine oxidase inhibitor, isatin, was also found to be a substrate for hAFAR with a K_m of $250 \mu\text{M}$ and a k_{cat} of 217 min^{-1} .

The data in Table 1 show two structural motifs can be identified in substrates that are reduced by AFAR proteins with relatively high catalytic efficiency; namely, carboxy-anion and aldehyde groups separated by 2 to 3 carbon atoms, and the presence of α -dicarbonyl groups on 5- and 6-membered rings.

The pH-dependence of catalysis by hAFAR for 2-CBA

Since 2-CBA is in equilibrium with its cyclic hemiacetal and this equilibrium is influenced by pH, we investigated the 2-CBA reductase activity of hAFAR at various pH conditions (Figure 6). Over the range from pH 5.3 to pH 8.4, the specific activity changed less than 2-fold, showing a significant decrease under basic conditions. The specific activity was relatively constant between pH 6 and 7. Since the same dependence of specific activity on pH was observed when activity was assayed with 9,10-PQ (results not shown), the ability to form a cyclic hemiacetal is unlikely to influence catalysis, but may instead reflect the requirement for a closely juxtaposed carbonyl group and an oxygen anion.

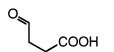
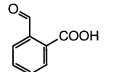
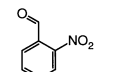
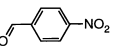
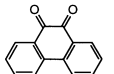
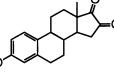
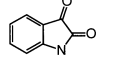
AFAR is the principal 2-CBA reductase in human liver

Western-blotting experiments carried out using antibodies raised against recombinant hAFAR showed the presence of a single immunoreactive band in human liver cytosol that co-migrated during SDS/PAGE with the immunogen. In total, 9 different specimens of human liver were examined, all of which contained broadly similar amounts of the unique 38 kDa cross-reacting protein (estimated as approx. 0.1%–0.2% of total soluble protein), indicating that marked interindividual variations in the hepatic levels of hAFAR do not commonly occur.

In order to determine the number of AKRs in human liver with activity towards 2-CBA, hepatic cytosol was subjected to anion-exchange chromatography on Q-Sepharose. By monitoring column eluate with not only 2-CBA, but also 9,10-PQ,

Table 1 Substrate specificity of recombinant human and rat AFAR proteins

The activities of hAFAR and rAFAR towards carbonyl-containing compounds were determined at 25 °C as described in the Materials and methods section using NADPH as cofactor. The kinetic constants were estimated from experiments that were performed on at least two separate occasions. Assays were carried out in duplicate, and Simple Fit with the Ultrafit curve-fitting programme was employed to calculate K_m and k_{cat} values from the initial reaction velocities obtained at five different substrate concentrations; the values shown represent mean \pm S.E.M. The K_m of human and rat AFAR for NADPH (last entry in the Table) was estimated with SSA as substrate.

Substrate	Enzyme	K_m (μ M)	k_{cat} (min^{-1})	k_{cat}/K_m ($\text{min}^{-1} \text{M}^{-1}$)
 succinic semialdehyde	hAFAR	15.4 \pm 2	92 \pm 3	6.0 $\times 10^6$
	rAFAR	184 \pm 33	69 \pm 8	3.8 $\times 10^5$
 2-carboxybenzaldehyde	hAFAR	20.0 \pm 1.2	101 \pm 5	5.1 $\times 10^6$
	rAFAR	0.76 \pm 0.3	74 \pm 4	9.7 $\times 10^7$
 2-nitrobenzaldehyde	hAFAR	2430 \pm 320	109 \pm 8	4.5 $\times 10^4$
	rAFAR	1100 \pm 21	490 \pm 5	4.5 $\times 10^5$
 4-nitrobenzaldehyde	hAFAR	6100 \pm 900	94 \pm 10	1.5 $\times 10^4$
	rAFAR	3600 \pm 1000	247 \pm 40	6.9 $\times 10^4$
 9,10-phenanthrenequinone	hAFAR	9.0 \pm 3.5	325 \pm 39	3.6 $\times 10^7$
	rAFAR	9.6 \pm 2.7	731 \pm 66	7.6 $\times 10^7$
 16-oxo-oestrone	hAFAR	40 \pm 6	142 \pm 10	3.6 $\times 10^6$
	rAFAR	24 \pm 5	518 \pm 42	2.2 $\times 10^7$
 isatin	hAFAR	248 \pm 31	217 \pm 16	8.8 $\times 10^5$
	rAFAR	105 \pm 87	87 \pm 29	8.3 $\times 10^5$
(with SSA) NADPH	hAFAR	0.75 \pm 0.3	108 \pm 9	1.4 $\times 10^8$
	rAFAR	0.32 \pm 0.14	91 \pm 10	2.8 $\times 10^8$

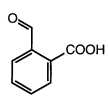
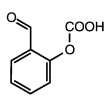
SSA and 4-NBA, it was found that carbonyl-reducing activity was resolved into nine peaks of enzyme activity. The elution profile shown in Figure 7 is a typical representative from a total of three separate analyses of liver specimen 666. These enzyme-containing peaks showed significant differences in their relative activities towards the four AKR substrates employed to assay the fractions. However, only Peak 6, which eluted between fractions 141 and 155, possessed 2-CBA reductase activity. Peak 6 also exhibited activity towards 9,10-PQ, SSA and 4-NBA, which is consistent with it containing hAFAR. Analysis of the protein in each of the reductase-containing peaks by Western blotting with antibody raised against recombinant hAFAR protein showed the presence of a strong immunoreactive 38 kDa polypeptide in Peak 6; some cross-reactivity with anti-hAFAR IgG was also observed in Peak 7, possibly due to carry-over, but the other peaks showed essentially no cross-reactivity with the antiserum. Antibodies against 3α -HSD used to probe the blot showed no cross-reactivity with proteins eluted in Peak 6, but did cross-react with a polypeptide of about 35 kDa that eluted in Peak 4.

These data suggest that hAFAR, or a protein co-eluting from Q-Sepharose with hAFAR, is responsible for the 2-CBA reductase activity in Peak 6. In order to determine which of these two possibilities is correct, the reductase in Peak 6 was purified in two affinity-chromatography steps, first on Matrex Orange A, and secondly on HiTrap Blue, as described in the Materials and methods section. From 1.5 g of human hepatic cytosol, 40 μ g of protein was isolated that had a specific activity towards 2-CBA of 1.75 μ mol/min/mg (Table 2). The purified enzyme cross-reacted strongly with anti-hAFAR IgG.

Sensitivity of AFAR to proteolysis *in vitro*

It was noted that whereas the single immunoreactive polypeptide in total liver cytosol had an apparent electrophoretic molecular mass of 38 kDa, two cross-reacting polypeptides with estimated molecular masses of 28 kDa and 12 kDa were observed in the combined Peak 6 fractions from Q-Sepharose and subsequent Matrex Orange A and Cibacron Blue pools (Figure 8). If the Q-Sepharose fractions were frozen immediately on elution from the anion exchanger, both full-length protein and cleaved proteins were detected by Western blotting. However, the protein was cleaved completely into polypeptides of 28 kDa and 12 kDa (apparent molecular mass) after storage of the fractions for 7 days at 4 °C, despite addition of the proteinase inhibitor Pefabloc to the liver cytosol. The 28 kDa polypeptide was subjected to automated Edman degradation, and yielded the sequence SRPPPPRVASV, indicating that it represented the N-terminal portion of the protein. Edman degradation of the 12 kDa fragment yielded the sequence GRFFGN(S)(W)AE which is equivalent to residues 220–229 of hAFAR (the numbering includes the initiator methionine). These data indicate that the two fragments are generated through cleavage of the Val²¹⁹–Gly²²⁰ peptide bond. It is also apparent that native hAFAR does not have a blocked N-terminus, and that the larger fragment produced by proteolysis has a molecular mass of 24.2 kDa, not 28 kDa (as inferred from SDS/PAGE).

The same susceptibility to proteolysis was observed with the recombinant hAFAR protein; extended storage of the thrombin-cleaved recombinant hAFAR at 4 °C resulted in the appearance of 28 kDa and 12 kDa polypeptides as secondary cleavage

Substrate (0.5 mM)	Relative activity
 2-carboxybenzaldehyde	100% ($K_m = 20 \mu\text{M}$)
 2-formylphenoxyacetic acid	30% ($K_m > 250 \mu\text{M}$)

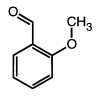
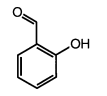
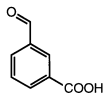
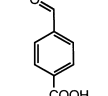
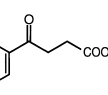
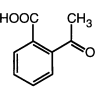
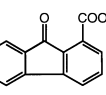
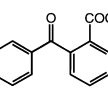
Relative activity $\leq 5\%$ of 2-CBA reductase activity			
 1.	 2.	 3.	 4.
 5.	 6.	 7.	 8.
Substrate (0.5^a or 1 mM^b)			
1. 2-methoxybenzaldehyde ^b	2. 2-hydroxybenzaldehyde ^a	3. 3-carboxybenzaldehyde ^b	4. 4-carboxybenzaldehyde ^b
5. 3-benzoylpropionic acid ^b	6. 2-acetylbenzoic acid ^a	7. 9-fluorenone-1-carboxylic acid ^a	8. 2-benzoylbenzoic acid ^a

Figure 5 Relative activities of hAFAR towards substrates that are structurally related to 2-CBA

Enzyme activity was determined as described in the Materials and methods section using NADPH as cofactor. Specific activities are reported as a percentage of that obtained with 2-CBA. Significant reductase activity was observed with 2-formylphenoxyacetic acid (30%), and modest reductase activity was found with 2-methoxybenzaldehyde (4%), 2-acetylbenzoic acid (5%), 9-fluorenone-1-carboxylic acid (2%) and 2-benzoylbenzoic acid (4%). The remaining four carbonyl-containing compounds showed less than 1% activity relative to 2-CBA.

products of the bacterially expressed protein. This thrombin-cleaved recombinant protein retained activity towards 9,10-PQ and 4-NBA equivalent to that of the full-length protein. The thrombin-cleavage site in the recombinant protein was mapped to Arg²²¹-Phe²²² by amino-acid sequencing of the 12 kDa peptide; 10 cycles of automated Edman degradation yielded the sequence FFGNSWAETY. The molecular mass of the two peptide fragments was calculated from primary structure and electrospray MS to be 24.70 and 12.27 kDa indicating, as discussed above, that the N-terminal peptide of 24.70 kDa migrates slightly anomalously during SDS/PAGE as a 28 kDa protein. Antibodies raised in two separate rabbits to recombinant protein were shown to be specific for either the 24.70 kDa N-terminal peptide (RW144) or the 12.27 kDa C-terminal peptide (RW143) of the recombinant cleaved protein; thus RW144 cross-reacted with the 28 kDa electrophoretic band, whereas RW143 cross-reacted with the 12 kDa electrophoretic band. These two antibodies showed a corresponding ability to detect both the putative N-terminal 28 kDa band and C-terminal 12 kDa band from human liver cytosol.

It should be noted that AFAR was purified on the basis of 2-

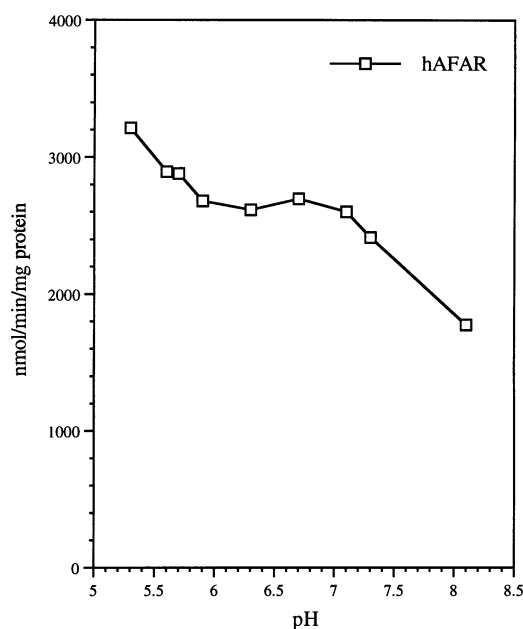


Figure 6 Dependence of 2-CBA reductase activity on pH

Activity towards 2-CBA was determined at pH values ranging from 5.3 to 8.4 using 100 mM sodium phosphate (adjusted to the desired pH with phosphoric acid). Values represent the average of duplicate measurements, which were found to vary by less than 5%.

CBA reductase activity, indicating that the reductase activity is maintained after proteolysis. It was therefore concluded that hAFAR is responsible for essentially all of the 2-CBA reductase activity in human liver, but that the enzyme is susceptible to cleavage *in vitro*, presumably due to co-purification of a proteinase that is insensitive to inhibition by Pefabloc. The enzyme responsible for cleavage of AFAR in human liver is probably not a serine proteinase because it was not inactivated by Pefabloc.

AFAR is expressed in all hepatocytes

Immunohistochemistry (Figure 9) demonstrated that antibodies against hAFAR gave positive cytoplasmic and nuclear staining in hepatocytes across normal human liver; staining appeared to be equally intense in zones 1, 2 and 3. The portal tract gave negative staining for AFAR. In primary biliary cirrhosis, AFAR was found to be present in hepatocyte regenerative nodules, but was absent from the intervening inflamed fibrous septa. No increased staining was observed in hepatocellular carcinoma.

AFAR is widely expressed in human tissues

In order to determine the specificity of expression of hAFAR, Northern-blot analysis was performed. Figure 10 shows that mRNA encoding AFAR can be detected in a wide range of human tissues. The highest signal was observed from kidney, pancreas, small intestine and skeletal muscle, whereas moderate amounts were found in liver, heart, testis and ovary. Lower levels of AFAR mRNA were observed in brain, colon, lung, prostate and thymus. Although barely detectable, a hybridization signal was seen in the RNA samples from spleen, leucocytes and placenta.

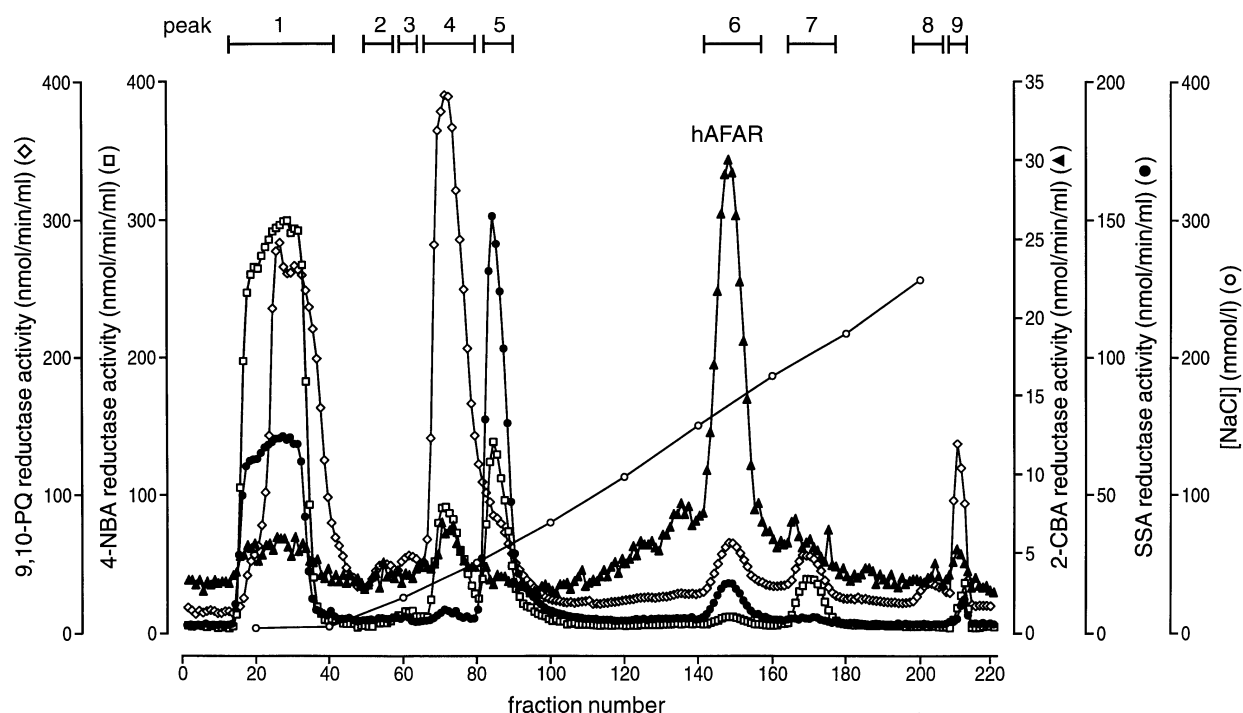


Figure 7 Resolution of the major human hepatic 2-CBA reductase from other AKRs

Human liver cytosol (1.5 g of protein) dialysed against buffer B was applied to a 2.5 cm × 45.0 cm column of Q-Sepharose. The anion exchanger was eluted at 30 ml/h and fractions of 8 ml were collected. The column was developed with a linear 1200 ml 0–250 mM NaCl gradient formed between fractions 35 and 205, after which the retained activity was eluted by the step-wise addition of 1 M NaCl. Reductase activity towards 2-CBA (▲), SSA (●), 4-NBA (□) and 9,10-PQ (◇) was measured as described in the text. The sodium concentration was measured using an ion-selective electrode, and is shown by open circles (○). The fractions which were combined for subsequent Western blotting and, in the case of peak 6, for enzyme purification are indicated by the horizontal bars.

Table 2 Purification of AFAR from human liver

See text for details.

Purification step	Total protein (mg)	Specific activity towards 2-CBA (nmol/min per mg)
Liver cytosol	1500	2
Q-Sepharose (peak 6)	35	63
HiTrap Blue	0.04	1750

DISCUSSION

The present paper describes the molecular cloning of a protein from human liver, which shares 78% sequence identity with the ethoxyquin-inducible AFAR from rat liver, and establishes the AFAR family (AKR7) within the superfamily of AKRs. This human protein, designated hAFAR, shares less than 20% identity with the human AKRs in the major AKR1 family, but shows more similarity in structure and sequence to the voltage-gated *Shaker*-related K⁺-channel β -subunit AKR6 family. The fact that both the rat and human AFAR proteins are distantly related to other AKR families might allow them to serve as valuable models to increase our understanding of the structure/function of the entire AKR superfamily. This possibility is currently of significance since recently, it has been proposed that the β -subunits of the voltage-gated K⁺-channels

are members of the AKR superfamily [8,24], although it remains to be established whether they possess catalytic activity.

Substrate specificity and *in vivo* function of hAFAR

Unlike aldose and aldehyde reductases, hAFAR exhibits a somewhat restricted substrate specificity that suggests a more specialized role in detoxification. Although used originally to identify rAFAR, aflatoxin is not a particularly good substrate for either rat or human AFAR. By comparison, hAFAR was found to possess three orders of magnitude greater specific activity for SSA than for AFB₁-dialdehyde. Human AFAR possesses a K_m of 15 μ M for SSA, suggesting that it may serve as a major SSA reductase *in vivo*. Under normal conditions, SSA produced from GABA metabolism by GABA-transaminase is metabolized by SSA dehydrogenase to succinic acid [51]. However, SSA will be metabolized in a tissue-specific fashion because the dehydrogenase is not ubiquitously expressed.

GABA-transaminase is widely distributed in non-neural tissues, including liver, lymphocytes, kidney, pancreas and testis, whereas SSA dehydrogenase may be absent from some of those tissues, such as pancreas and testis [52,53]. This raises the possibility that hAFAR may function as an SSA reductase in those tissues deficient in SSA dehydrogenase. Cases of genetic SSA dehydrogenase deficiency [54] serve to illustrate that reduction of SSA is a significant *in vivo* pathway, and does occur in the absence of SSA dehydrogenase, as witnessed by the observed 4-hydroxybutyric aciduria in these patients.

Early attempts to characterize SSA reductase from human brain identified an enzyme with features similar to those of

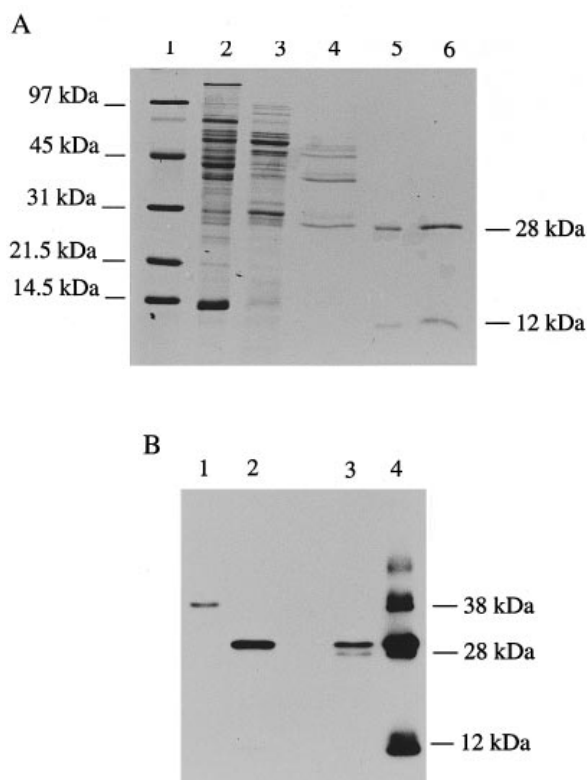


Figure 8 Purification of 2-CBA reductase from human liver

The Q-Sepharose fractions containing the major peak of 2-CBA reductase activity from human liver cytosol were combined and subjected sequentially to affinity chromatography on Matrex Orange A followed by affinity chromatography on immobilized Cibacron Blue. (A) shows SDS/PAGE analysis of the protein recovered at each of the stages of purification. The gel, which was stained with Coomassie Blue, was loaded as follows: 1, protein molecular mass standards; 2, human liver cytosol; 3, combined fractions 141–155 from Q-Sepharose (Figure 7); 4, pool from Matrex Orange A; 5, purified material from HiTrap Blue; 6, $2 \times$ protein from HiTrap Blue that was loaded in lane 5. (B) shows an AFAR-immunoblot analysis of the following samples: 1, hepatic cytosol; 2, Q-Sepharose peak 6; 3, peak 6 protein eluted from Matrex Orange A; 4, purified hAFAR from HiTrap Blue.

hAFAR; both proteins are anionic, exhibit a relative preference for SSA over 4-NBA, and possess similar K_m values for SSA ($15 \mu\text{M}$) and NADPH ($4 \mu\text{M}$) [55]. As hAFAR is expressed in cerebellum, it is possible that it is identical to SSA reductase described by Hoffman et al. [55]. However, the SSA reductase purified by these workers was thought to be a dimeric protein with a native molecular mass of 78 kDa. By contrast, the molecular mass of native hAFAR estimated by gel filtration on Superose FPLC is approximately 50 kDa, whereas the subunit molecular mass calculated by SDS/PAGE is 38 kDa. The discrepancy between the molecular masses of hAFAR under native and denaturing conditions may reflect a tendency for it to aggregate. Clearly, further work is required to establish the identity of the major brain SSA reductase. It is, however, apparent from the Q-Sepharose elution profile shown in Figure 7 that hAFAR does not represent the major SSA reductase in human liver.

A search for anionic aldehyde substrates similar to SSA and the dialdehydic form of AFB₁-8,9-dihydrodiol resulted in the identification of hAFAR as a 2-CBA reductase, an activity of pharmacological relevance with respect to the reduction of phthalidyl esters *in vivo*. Further examination of a series of

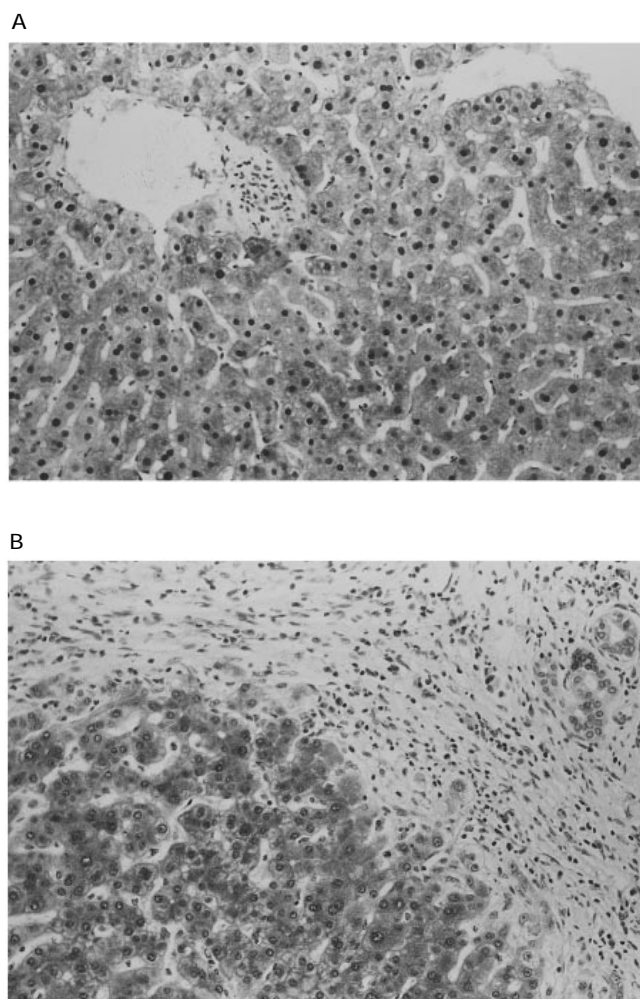


Figure 9 Immunohistochemical localization of hAFAR in human liver

Formalin-fixed sections of liver were reacted with anti-hAFAR serum, and the immunoreactive material detected using horseradish peroxidase and 3,3-diaminobenzidine. Normal liver (A) showed cytoplasmic and nuclear hepatocyte staining throughout the liver, with negative staining of the portal tract (top left). Primary biliary cirrhotic liver (B) showed staining in hepatocyte regenerative nodules, but not in intervening inflamed fibrous septa (top right). Magnification was $\times 300$.

compounds structurally related to 2-CBA (Table 1 and Figure 5) demonstrated that hAFAR only significantly reduced 2-CBA and the related 2-formylphenoxyacetic acid; the metabolism *in vivo* of carboxy-substituted benzaldehydes described by Shiobara [29] correlates with the substrate specificity of hAFAR *in vitro*.

Predicted structure of AFAR proteins

Computer-assisted predictions of the secondary structure of hAFAR and rAFAR suggested that these two proteins may adopt a similar fold to that demonstrated by X-ray crystallography for ALDR [38,39,56] and 3- α HSD [57]. This approach allowed the identification of ten putative α -helical elements and nine β -sheet elements in the human and rat AFAR proteins. The alignment was compared with the tertiary structure of ALDR in order to confirm that important catalytic, NADPH-binding and

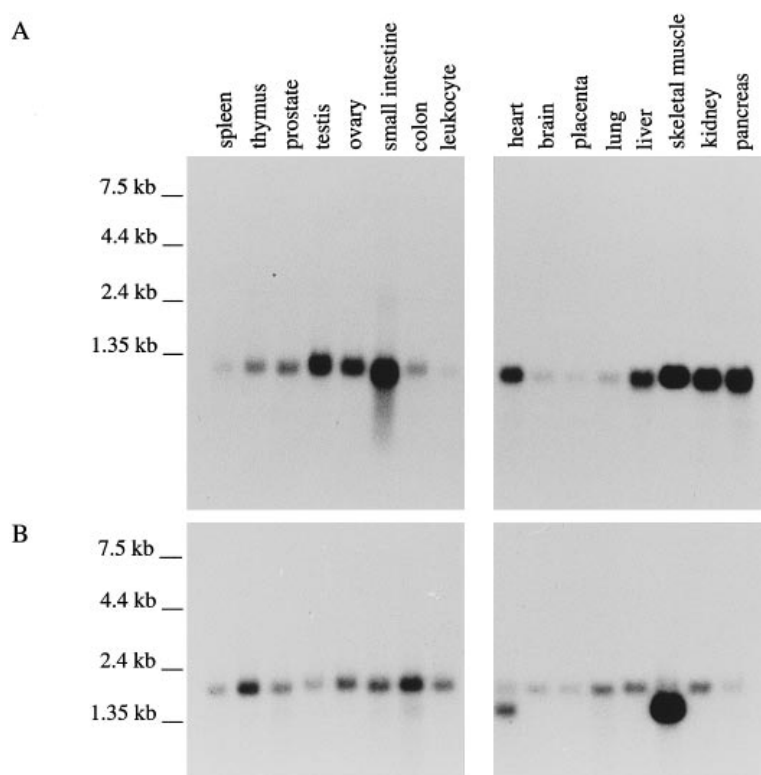


Figure 10 Distribution of hAFAR in human tissues

Size-fractionated RNA tissue blots were probed with: (A) the *EcoRI/BglII* fragment of pL118, and (B) the β -actin cDNA provided by Clontech in their Multiple Tissue Northern Blot kit.

hydrophobic residues were aligned with putative equivalent residues in the AFAR proteins (Figure 2). Two major differences in the predicted topology of the AFAR proteins and the crystal structure of ALDR were apparent using this method. First, loop A of ALDR, between Pro¹¹⁷ and Ile¹³⁷, was not represented in either of the AFAR proteins (this would be located between Pro¹¹⁹ and Val¹²⁰ of hAFAR). Secondly, the region between S9 and H8 of ALDR, which includes the NADPH-enfolding loop B, is replaced by a markedly different structure in hAFAR. The loop B of ALDR is located at the exposed surface of the protein and undergoes a large conformational change on binding NADPH, thus contributing to the tight binding of cofactor that typifies the AKR family [58,59]. In addition to contributing Trp²¹⁹ to the substrate-binding pocket, loop B also contains residues that interact with the NADPH pyrophosphate bridge. The corresponding residues in the AFAR proteins (Ala²⁰⁰–Asp²¹⁴) are not conserved, and it is therefore not possible to assign a function to specific residues on the basis of the ALDR crystal structure. Nevertheless, this region of AFAR is much more similar to the K⁺-channel β -subunit (67% similar) than to ALDR (no obvious similarity), and may represent an alternative way of interacting with the NADPH-pyrophosphate bridge. Juxtaposed to the extended loop B, this alignment predicts the presence of an additional α -helix comprising 29 residues which can be aligned with an α -helix of similar length in the K⁺-channel β -subunit (Figure 2). Previous alignments [24] have not taken into account the predicted secondary structure of the AFAR and β -subunit proteins.

The preference of hAFAR for substrates with a carboxylate anion closely spaced to the reactive carbonyl suggests that, like ALDR, the active site contains an anion-binding site [56]. The

overall conservation of many of the ALDR active-site residues which form part of the catalytic triad, or interact with the nicotinamide and adenine moieties of NADPH, suggests that the geometry of the cofactor-binding site is similar in AKR7 and AKR1 proteins. However, few of the residues which form the substrate pocket in ALDR are conserved in hAFAR, and the predicted substitution of polar for hydrophobic residues (Figure 2) is consistent with the preference of hAFAR for charged substrates. Further work is required to define the significance of the substitutions of the residues in the substrate pocket of AKR1 proteins in terms of the specificity of AKR7 for 2-CBA and SSA.

The human *Shaker*-related K⁺-channel β -subunit described by England et al. [21] was included in the alignment shown in Figure 2 as the human member of the AKR family (AKR6) that is most similar to the AFAR protein family (AKR7). Like AFAR, the β -subunit shows high conservation of the residues which comprise the ALDR catalytic triad, as well as those which interact with nicotinamide and adenine (Table 3). Comparison of the AFAR proteins with the β -subunit shows that the K⁺-channel protein also lacks loop A and, like AFAR, is predicted to contain an additional α -helix flanking the loop B/NADPH-enfolding region of ALDR. There are further similarities between the AFAR proteins and the β -subunit in the length and sequence of the predicted α -helix that replaces loop C. Overall, the similarity of AFAR proteins and β -subunits raises questions about possible roles of both proteins in ligand-gated signal-transduction pathways.

Both native hAFAR and the recombinant enzyme were found to be susceptible to proteolysis at a site flanking the 29-residue AFAR α -helix. Native hAFAR was found to be susceptible to proteolysis, and during purification from human liver gave two

Table 3 Amino acids in hAFAR proteins and K⁺-channel β -subunits that align with residues in aldose reductase involved in cofactor and substrate binding.

The amino acids in hAFAR which are listed are those that are conserved in ALDR and are believed (from the crystal structure of the latter reductase) to contribute to catalysis ([38] and [39]). The numbering of amino acids for hAFAR, rAFAR and the β -subunit includes the initiator methionine. However, the numbering of residues in ALDR excludes the initiator methionine.

hAFAR	rAFAR	β -subunit	ALDR	Secondary structure in ALDR	Function in ALDR
Asp ⁴³	Asp ⁴⁰	Asp ¹²⁶	Asp ⁴³	S4	Hydrogen bonding with the 2-OH group of the nicotinamide ribose unit of NADPH and Lys ⁷⁷
Tyr ⁴⁸	Tyr ⁴⁵	Tyr ¹³¹	Tyr ⁴⁸	-	Candidate catalytic acid
Lys ⁷⁶	Lys ⁷³	Lys ¹⁵⁹	Lys ⁷⁷	S5	Hydrogen bonding with active-site Tyr ⁴⁸
His ¹¹²	His ¹⁰⁹	Asn ¹⁹⁹	His ¹¹⁰	-	Involved in hydrogen bond formation either with hydroxyl of Tyr ⁴⁸ or with oxygen of bound substrate, and may participate in proton donation
Ser ¹⁴²	Ser ¹³⁹	Ser ²²⁹	Ser ¹⁵⁹	S7	Hydrogen bonding with carboxamide moiety of nicotinamide ring
Asn ¹⁴³	Asn ¹⁴⁰	Arg ²³⁰	Asn ¹⁶⁰	S7	Hydrogen bonding with carboxamide moiety of nicotinamide ring
Gln ¹⁶⁸	Gln ¹⁶⁵	Gln ²⁵⁵	Gln ¹⁸³	S8	Hydrogen bonding with carboxamide moiety of nicotinamide ring
Tyr ¹⁹⁶	Phe ¹⁹³	Trp ²⁸⁴	Tyr ²⁰⁹	S9	Shares its π -electrons with the B-face of the nicotinamide ring (π -stacking) such that the A face can deliver the hybrid ion with 4- <i>pro</i> -R stereochemistry
Ser ²⁹⁰	Ser ²⁸⁷	Thr ³⁶⁷	Thr ²⁶⁵	-	Hydrogen bonding with 2'-monophosphate of 2'-AMP
Asn ²⁹⁷	Asn ²⁹⁴	Asn ³⁷⁴	Asn ²⁷²	H9	Hydrogen bonding with the amino group at C6 in adenine

fragments generated by cleavage at the peptide bond between Val²¹⁹ and Gly²²⁰. Heterologously expressed hAFAR, that had been thrombin-cleaved to remove the polyhistidine tag and stored for several weeks, yielded 2 peptides: the internal cleavage site in hAFAR isolated from *E. coli* was determined to be the peptide bond between Arg²²¹ and Phe²²². Both the Val²¹⁹-Gly²²⁰ and the Arg²²¹-Phe²²² peptide bonds, which are subject to proteolysis, lie within the extended 'loop B' region described above. Surprisingly, it was found that the cleaved enzyme retained activity towards 9,10-PQ, 4-NBA and 2-CBA, but not SSA, presumably indicating that proteolysis results in a conformational change in hAFAR that allows it to reduce aromatic compounds while losing activity towards small carbonyls. The physiological significance, if any, of susceptibility of AFAR proteins to proteolysis is unclear, but it is possible that it is advantageous to the cell to regulate certain activities of this enzyme.

Fractionation of hepatic carbonyl-reducing activity

Fractionation of total hepatic carbonyl-reducing activity by anion-exchange chromatography on Q-Sepharose has resolved nine peaks of carbonyl-reductase activity. Where indicated in the text, additional substrates and assay conditions were used to help with the identification of individual peaks. The major hepatic carbonyl-reducing enzymes carbonyl reductase, 3 α -HSD and aldehyde reductase can be tentatively identified by their substrate specificity and order of elution from the anion-exchange column (see Figure 7). The large flow-through peak labelled as peak 1 contains carbonyl reductase, on the basis of substrate specificity for 9,10-PQ, 4-NBA and SSA [60–62]. Peaks 2 and 3 are relatively minor, possessing a small amount of activity with only 9,10-PQ, and their identity is unknown. Peak 4 contains 3 α -HSD, as identified by activity with both 9,10-PQ [47] and acenaphthenol (results not shown) [11,16], as well as its immunoreactivity with antibodies against the DD encoded by the cDNA clone c32. Peak 5 is thought to contain aldehyde reductase, as demonstrated by activity towards SSA and 4-NBA [55,63]. Further testing of peak 5 indicated a complete lack of NADH-dependent reductase activity (results not shown), consistent with the identification of this activity as aldehyde reductase [64]. The major 2-CBA-reductase peak corresponded to peak 6, which was shown to contain hAFAR by Western blotting using antibodies raised to

recombinant hAFAR (Figure 8B). The 2-CBA reductase activity co-purified with hAFAR during subsequent affinity-chromatography steps. The identity of the remaining enzyme-containing peaks 7, 8 and 9 is less certain.

Previous workers have used Q-Sepharose chromatography to resolve multiple forms of human hepatic dehydrogenase activity towards benzene dihydrodiol [62,65]. These peaks of DD activity have been designated DD1, DD2, DD3 and DD4, according to their order of elution from the anion-exchange column. The identity of DD1–DD4 when compared with other AKRs is uncertain, though DD3 has been proposed to be aldehyde reductase (identified as peak 5 in Figure 7) because of its high activity with D-glucuronate and its immunochemical properties [62,65]. On the basis of elution position and acenaphthenol activity, DD1 and DD2 appear to be equivalent to peaks 1 and 4 respectively, shown in Figure 7. It is likely that the DD4 peak is equivalent to chlordecone reductase (Type I 3 α -HSD [16]) which appears to be highly variable since inter-individual differences in the amount of this protein in human liver have been described [66] and Southern blots have shown inter-individual differences in genomic DNA restriction fragments that hybridize to the chlordecone reductase cDNA [10]. The correlation, if any, of DD4 with the unidentified peaks 7–9 requires further investigation, and we are currently developing antibodies to allow the unequivocal identification of chlordecone reductase in our profiles.

Concluding comments

The human and rat AFAR proteins appear to be subject to distinct regulatory mechanisms. Northern-blotting experiments demonstrated that hAFAR is widely expressed in human tissues, whereas in the rat, rAFAR is constitutively expressed in kidney, but is essentially absent from the liver, lung and brain. Expression of the rat AFAR protein in the liver is inducible by a variety of synthetic antioxidants including ethoxyquin, butylated hydroxyanisole and oltipraz [18,48]. In contrast, we have found constitutive expression of hAFAR in hepatic cytosol; immuno-histochemical studies of hAFAR have indicated that it is evenly expressed across the zones of human liver. Lastly, hAFAR does not appear to be overexpressed in human hepatocellular carcinomas, whereas the rAFAR protein is overexpressed in rat liver pre-neoplastic nodules and in hepatomas. It is likely that

further members of the AKR7 family exist in the human and therefore, at present, it cannot be stated categorically that inducible AFAR-like proteins are not present in man.

This paper describes the structure, catalytic properties and tissue distribution of hAFAR, a novel member of the AKR7 family of AKRs. It is proposed that possession of an extended 'loop B' region juxtaposed to an additional α -helix reflects a different type of interaction with the cofactor NADPH, which is shared by the AKR6 family represented by the β -subunits of the voltage-gated K^+ -channels. At a functional level, the human and rat AFAR proteins are distinguishable from other reductases because of their activities towards AFB₁-dialdehyde and 2-CBA. The surprisingly low K_m for SSA suggests that human AFAR could function both as an SSA reductase and as a 2-CBA reductase *in vivo*. Analysis of total 2-CBA reductase activity in human liver indicates that, indeed, hAFAR represents the major hepatic reductase for this carbonyl-containing compound.

This work was supported by Medical Research Council Grant G9322073PA, and the centrifugal analyser was purchased with a Scottish Office Home and Health Department equipment grant K/SCO/2/20/3/7. Dr. Ken Tew is thanked for providing the c32 clone for DD. We gratefully acknowledge the expert help of Mr. David J. Judah in performing the aflatoxin enzyme assays, Dr. Andrew D. Cronshaw for carrying out the amino-acid sequencing experiments, Mr. Vincent P. Kelly for preparing peptides for sequencing, and Ms. Tania O'Connor for providing antibodies against 3α -HSD. Finally, Dr. Dave K. Wilson is thanked for constructive criticism and discussions.

REFERENCES

- Penning, T. (1993) *Chem. Biol. Interact.* **89**, 1–34
- Wang, X. P., Sheikh, S., Saigal, D., Robinson, L. and Weiner, H. (1996) *J. Biol. Chem.* **271**, 31172–31178
- Yoshihara, S. and Tatsumi, K. (1997) *Arch. Biochem. Biophys.* **338**, 29–34
- Lieber, C. S. (1994) *J. Toxicol. Clin. Toxicol.* **32**, 631–681
- Maser, E. (1995) *Biochem. Pharmacol.* **49**, 421–440
- Li, R., Bianchet, M. A., Talalay, P. and Amzel, L. M. (1995) *Proc. Natl. Acad. Sci. U.S.A.* **92**, 8846–8850
- Hayes, J. D. and Pulford, D. J. (1995) *Crit. Rev. Biochem. Mol. Biol.* **30**, 445–600
- Jez, J. M., Flynn, T. G. and Penning, T. M. (1997) *Biochem. Pharmacol.* **54**, 639–647
- Bohren, K. M., Bullock, B., Wermuth, B. and Gabbay, K. H. (1989) *J. Biol. Chem.* **264**, 9547–9551
- Winters, C. J., Molowa, D. T. and Guzelian, P. S. (1990) *Biochemistry* **29**, 1080–1087
- Stolz, A., Hammond, L., Lou, H., Takikawa, H., Ronk, M. and Shively, J. E. (1993) *J. Biol. Chem.* **268**, 10448–10457
- Qin, K.-N., New, M. I. and Cheng, K.-C. (1993) *J. Steroid Biochem. Mol. Biol.* **46**, 673–679
- Kondo, K. H., Kai, M. H., Setoguchi, Y., Eggertsen, G., Sjoblom, P., Setoguchi, T., Okuda, K. I. and Bjorkhm, I. (1994) *Eur. J. Biochem.* **219**, 357–363
- Ciaccio, P. J. and Tew, K. D. (1994) *Biochim. Biophys. Acta* **1186**, 129–132
- Deyashiki, Y., Ogasawara, A., Nakayama, T., Nakanishi, M., Miyabe, Y., Sato, K. and Hara, A. (1994) *Biochem. J.* **299**, 545–552
- Khanna, M., Qin, K.-N., Wang, R. W. and Cheng, K.-C. (1995) *J. Biol. Chem.* **270**, 20162–20168
- Hara, A., Matsuura, K., Tamada, Y., Sato, K., Miyabe, Y., Deyashiki, Y. and Ishida, N. (1996) *Biochem. J.* **313**, 373–376
- Hayes, J. D., Judah, D. J. and Neal, G. E. (1993) *Cancer Res.* **53**, 3887–3894
- Ellis, E. M., Judah, D. J., Neal, G. E. and Hayes, J. D. (1993) *Proc. Natl. Acad. Sci. U.S.A.* **90**, 10350–10354
- Rettig, J., Heinemann, S. H., Wunder, F., Lorra, C., Parcej, D. N., Dolly, J. O. and Pongs, O. (1994) *Nature (London)* **369**, 289–294
- England, S. K., Uebele, V. N., Shear, H., Kodali, J., Bennett, P. B. and Tamkun, M. M. (1995) *Proc. Natl. Acad. Sci. U.S.A.* **92**, 6309–6313
- Morales, M. J., Castellino, R. C., Crews, A. L., Rasmusson, R. L. and Strauss, H. C. (1995) *J. Biol. Chem.* **270**, 6272–6277
- Leicher, T., Roeper, J., Weber, K., Wang, X. and Pongs, O. (1996) *Neuropharmacology* **35**, 787–795
- McCormack, T. and McCormack, K. (1994) *Cell* **79**, 1133–1135
- McMahon, R. E. (1982) in *Metabolic Basis of Detoxication* (Jakoby, W. B., Bend, J. R. and Caldwell, J., eds.), pp. 91–104, Academic Press, New York
- Shiobara, Y. and Ogiso, T. (1979) *Xenobiotica* **9**, 157–164
- Jaffe, G., Murphy, J. E. and Robinson, O. P. (1976) *Practitioner* **216**, 455–460
- Moss, J. and Bundgaard, H. (1992) *Acta Pharm. Nord.* **4**, 301–308
- Shiobara, Y. (1977) *Xenobiotica* **7**, 457–468
- Tonda, K., Kamata, S. and Hirata, M. (1987) *Xenobiotica* **17**, 759–768
- Tonda, K. and Hirata, M. (1992) *Xenobiotica* **22**, 691–699
- Adams, M. D., Dubnick, M., Kerlavage, A. R., Moreno, R., Kelley, J. M., Utterback, T. R., Nagle, J. W., Fields, C. and Venter, J. C. (1992) *Nature (London)* **355**, 632–634
- Sambrook, J., Fritsch, E. F. and Maniatis, T. (1989) *Molecular Cloning: A Laboratory Manual*, 2nd edn., Cold Spring Harbor Laboratory Press, Cold Spring Harbor, New York
- Sanger, F., Nicklen, S. and Coulson, A. R. (1977) *Proc. Natl. Acad. Sci. U.S.A.* **74**, 5463–5467
- Allschul, S. F., Gish, W., Miller, W., Myers, E. W. and Lipman, D. J. (1990) *J. Mol. Biol.* **215**, 403–410
- Sander, C. and Schneider, R. (1991) *Proteins* **9**, 56–68
- Rost, R. and Sander, C. (1993) *J. Mol. Biol.* **232**, 584–599
- Wilson, D. K., Bohren, K. M., Gabbay, K. H. and Quioccho, F. A. (1992) *Science* **257**, 81–84
- Wilson, D. K., Tarle, I., Petrash, J. M. and Quioccho, F. A. (1993) *Proc. Natl. Acad. Sci. U.S.A.* **90**, 9847–9851
- Ellis, E. M. and Hayes, J. D. (1995) *Biochem. J.* **312**, 535–541
- Bradford, M. M. (1976) *Anal. Biochem.* **72**, 248–254
- Laemmli, U.K. (1970) *Nature (London)* **227**, 680–685
- Hayes, J. D., Kerr, L. A. and Cronshaw, A. D. (1989) *Biochem. J.* **264**, 437–445
- Hayes, J. D., Judah, D. J., McLellan, L. I., Kerr, L. A., Peacock, S. D. and Neal, G. E. (1991) *Biochem. J.* **279**, 385–398
- Bohren, K. M., Grimshaw, C. E. and Gabbay, K. H. (1992) *J. Biol. Chem.* **267**, 20965–20970
- Cromlish, J. A., Yoshimoto, C. K. and Flynn, T. G. (1985) *J. Neurochem.* **44**, 1477–1484
- Pawlowski, J. E. and Penning, T. M. (1994) *J. Biol. Chem.* **269**, 13502–13510
- Ellis, E. M., Judah, D. J., Neal, G. E., O'Connor, T. and Hayes, J. D. (1996) *Cancer Res.* **56**, 2758–2766
- Fletcher, D. A., McMeeking, R. F. and Parkin, D. (1996) *J. Chem. Inf. Comput. Sci.* **36**, 746–749
- Fujita, T. and Nishioka, T. (1976) *Prog. Phys. Org. Chem.* **12**, 49–89
- Chambliss, K. L. and Gibson, K. M. (1992) *Int. J. Biochem.* **24**, 1493–1499
- Tillakaratne, N. J. K., Medina-Kauwe, L. and Gibson, K. M. (1995) *Comp. Biochem. Physiol.* **112A**, 247–263
- Chambliss, K. L., Zhang, Y. A., Rossier, E., Vollmer, B. and Gibson, K. M. (1995) *J. Neurochem.* **65**, 851–855
- Hoffmann, G. F., Gibson, K. M., Trefz, F. K., Nyhan, W. L., Bremer, H. J. and Rating, D. (1994) *Eur. J. Pediatr.* **153**, S94–S100
- Hoffman, P. L., Wermuth, B. and von Wartburg, J. P. (1980) *J. Neurochem.* **35**, 354–366
- Harrison, D. H., Bohren, K. M., Ringe, D., Petsko, G. A. and Gabbay, K. H. (1994) *Biochemistry* **33**, 2011–2020
- Hoog, S., Pawlowski, J. E., Alzari, P. M., Penning, T. M. and Lewis, M. (1994) *Proc. Natl. Acad. Sci. U.S.A.* **91**, 2517–2521
- Grimshaw, C. E. (1992) *Biochemistry* **31**, 10139–10145
- Borhani, D. W., Harter, T. M. and Petrash, J. M. (1992) *J. Biol. Chem.* **267**, 24841–24847
- Wermuth, B., Platts, K. L., Seidel, A. and Oesch, F. (1986) *Biochem. Pharmacol.* **35**, 1277–1282
- Iwata, N., Inazu, N., Hara, S., Yanase, T., Kano, S., Endo, T., Kuriwaga, F., Sato, Y. and Satoh, T. (1993) *Biochem. Pharmacol.* **45**, 1711–1714
- Ohara, H., Miyabe, Y., Deyashiki, Y., Matsuura, K. and Hara, A. (1995) *Biochem. Pharmacol.* **50**, 221–227
- Bohren, K. M., Page, J. L., Shanker, R., Henry, S. P. and Gabbay, K. H. (1991) *J. Biol. Chem.* **266**, 24031–24037
- Wermuth, B., Munch, J. D. B. and von Wartburg, J.-P. (1977) *J. Biol. Chem.* **252**, 3821–3828
- Hara, A., Taniguchi, H., Nakayama, T. and Sawada, H. (1990) *J. Biochem.* **108**, 250–254
- Molowa, D. T., Shayne, A. G. and Guzelian, P. S. (1986) *J. Biol. Chem.* **261**, 12624–12627